

THE INCREMENTAL DYNAMIC ANALYSIS AND ITS APPLICATION TO PERFORMANCE-BASED EARTHQUAKE ENGINEERING

Dimitrios Vamvatsikos¹ and C. Allin Cornell²

¹Graduate Student, Department of Civil and Environmental Engineering, Stanford University, CA 94305-4020

²Professor, Department of Civil and Environmental Engineering, Stanford University, CA 94305-4020

ABSTRACT

Incremental Dynamic Analysis (IDA) is an emerging analysis method that offers thorough seismic demand and capacity prediction capability by using a series of nonlinear dynamic analyses under a multiply scaled suite of ground motion records. Realization of its opportunities requires several innovations, such as choosing suitable ground motion Intensity Measures (*IMs*) and representative Damage Measures (*DMs*). In addition, proper interpolation and summarization techniques for multiple records need to be employed, providing the means for estimating the probability distribution of the structural demand given the seismic intensity. Limit-states, such as the dynamic global system instability, can be naturally defined in the context of IDA, thus allowing annual rates of exceedance to be calculated. Finally, the data gathered through IDA can provide intuition for the behavior of structures and shed new light on the connection between the Static Pushover (SPO) and the dynamic response. To illustrate all the above concepts, a complete walkthrough of the methodology is presented by using a 9-storey steel moment-resisting frame with fracturing connections as an example to explain and clarify the application of the IDA to Performance-Based Earthquake Engineering (PBEE).

Keywords: performance-based earthquake engineering, incremental dynamic analysis, demand, collapse capacity, limit-state, nonlinear dynamic analysis, static pushover

INTRODUCTION

An important issue in Performance-Based Earthquake Engineering is the estimation of structural performance under seismic loads, in particular the estimation of the mean annual rate of exceeding a specified level of structural demand (e.g., maximum peak interstorey drift ratio θ_{\max}) or a certain limit-state capacity (e.g., global dynamic instability). A promising method that has recently risen to meet these needs is Incremental Dynamic Analysis (IDA), which involves performing nonlinear dynamic analyses of the structural model under a suite of ground motion records, each scaled to several intensity levels designed to force the structure all the way from elasticity to final global dynamic instability (Vamvatsikos and Cornell [1]). Thus, we can generate IDA curves of the structural response, as measured by a Damage Measure

TABLE 1
SET OF GROUND MOTION RECORDS

No	Event	Station	ϕ° ¹	Soil ²	M ³	R ⁴ (km)	PGA (g)
1	Loma Prieta, 1989	Agnews State Hospital	090	C,D	6.9	28.2	0.159
2	Imperial Valley, 1979	Plaster City	135	C,D	6.5	31.7	0.057
3	Loma Prieta, 1989	Hollister Diff. Array	255	-,D	6.9	25.8	0.279
4	Loma Prieta, 1989	Anderson Dam Downstream	270	B,D	6.9	21.4	0.244
5	Loma Prieta, 1989	Coyote Lake Dam Downstream	285	B,D	6.9	22.3	0.179
6	Imperial Valley, 1979	Cucapah	085	C,D	6.5	23.6	0.309
7	Loma Prieta, 1989	Sunnyvale Colton Ave	270	C,D	6.9	28.8	0.207
8	Imperial Valley, 1979	El Centro Array #13	140	C,D	6.5	21.9	0.117
9	Imperial Valley, 1979	Westmoreland Fire Station	090	C,D	6.5	15.1	0.074
10	Loma Prieta, 1989	Hollister South & Pine	000	-,D	6.9	28.8	0.371
11	Loma Prieta, 1989	Sunnyvale Colton Ave	360	C,D	6.9	28.8	0.209
12	Superstition Hills, 1987	Wildlife Liquefaction Array	090	C,D	6.7	24.4	0.180
13	Imperial Valley, 1979	Chihuahua	282	C,D	6.5	28.7	0.254
14	Imperial Valley, 1979	El Centro Array #13	230	C,D	6.5	21.9	0.139
15	Imperial Valley, 1979	Westmoreland Fire Station	180	C,D	6.5	15.1	0.110
16	Loma Prieta, 1989	WAHO	000	-,D	6.9	16.9	0.370
17	Superstition Hills, 1987	Wildlife Liquefaction Array	360	C,D	6.7	24.4	0.200
18	Imperial Valley, 1979	Plaster City	045	C,D	6.5	31.7	0.042
19	Loma Prieta, 1989	Hollister Diff. Array	165	-,D	6.9	25.8	0.269
20	Loma Prieta, 1989	WAHO	090	-,D	6.9	16.9	0.638

¹ Component ² USGS, Geomatrix soil class ³ moment magnitude ⁴closest distance to fault rupture

(DM , e.g., peak roof drift or maximum peak interstorey drift θ_{\max}), versus the ground motion intensity level, measured by an Intensity Measure (IM , e.g., peak ground acceleration or the 5%-damped first-mode spectral acceleration $S_a(T_1, 5\%)$). In turn these can be processed and summarized to get the distribution of demand DM given intensity IM . Additionally, limit-states (e.g., Immediate Occupancy or Collapse Prevention [2]) can be defined on each IDA curve and summarized to produce the probability of exceeding a specified limit-state given the IM level. The final results are in a suitable format to be conveniently integrated with a conventional hazard curve in order to calculate annual rates of exceeding a certain limit-state capacity, or a certain demand.

While it is a simple concept, performing an IDA involves important issues that need to be dealt with and requires several innovations to ease the computational burden. Based on the background and theory for IDA as established by Vamvatsikos and Cornell [1], we are going to touch upon the basics of the method, walk the reader through a practical example of its application and explain the tools we use to automate the calculations needed for IDA.

PRELIMINARIES: MODEL AND GROUND MOTION RECORDS

To illustrate our methodology, we will use a centreline model of a 9-storey steel-moment resisting frame designed for Los Angeles according to the 1997 NEHRP provisions (Lee and Foutch [3]). The model has a first-mode period of $T_1 = 2.3$ sec and it incorporates ductile members, shear panels and realistically fracturing Reduced Beam Section connections, while it includes the influence of interior gravity columns and a first-order treatment of global geometric nonlinearities (P- Δ effects).

In addition we need a suite of ground motion records. Previous studies [4] have shown that

for mid-rise buildings, ten to twenty records are usually enough to provide sufficient accuracy in the estimation of seismic demands, assuming a relatively efficient *IM*, like $S_a(T_1, 5\%)$, is used. Consequently, we have selected a set of twenty ground motion records, listed in Table 1, that belong to a bin of relatively large magnitudes of 6.5–6.9 and moderate distances, all recorded on firm soil and bearing no marks of directivity; effectively they represent a scenario earthquake.

PERFORMING THE ANALYSIS

Once the model has been formed and the ground motion records have been selected, we need a fast and automated way to perform the actual dynamic analyses needed for IDA. This entails appropriately scaling each record to cover the entire range of structural response, from elasticity, to yielding, and finally global dynamic instability. Our task is made significantly easier by using an advanced algorithm, like *hunt & fill* [1]. This ensures that the record scaling levels are optimally selected to minimize the number of required runs: Analyses are performed at rapidly increasing levels of *IM* until numerical non-convergence is encountered (signalling global dynamic instability), while additional analyses are run at intermediate *IM*-levels to sufficiently bracket the global collapse and increase the accuracy at lower *IM*s. The user only needs to specify the desired accuracy for demand and capacity, select the maximum tolerable number of dynamic analyses, and then wait for a few hours to get the results. Since the algorithm has been implemented in software [5] able to wrap around most existing analysis programs (e.g., DRAIN-2DX) it renders IDA almost effortless, needing no human supervision.

Regarding the computational cost, obviously, the more the analyses per record, the better the accuracy and the longer for IDA to complete. Still, with the use of such advanced algorithms no runs are wasted, thus ten runs per record will suffice to strike a good compromise between speed and accuracy. Nevertheless, sceptics would point out that performing 200 dynamic runs for a model with thousands of degrees-of-freedom is a daunting task. Yet, even for such a complicated model, it only took about 12 hours on two 1998-era Pentium-class processors running in parallel. The process is completely automated and so easily performed overnight that actually setting up the structural model can now be expected to take substantially more time than doing the analysis, and computer time is becoming an ever-cheaper commodity.

POSTPROCESSING

Equally important to the analysis is the postprocessing of the resulting data and perhaps the most important issue here is selecting a suitable *IM* and *DM*. There are several issues of efficiency and sufficiency associated with the *IM* selection [6]. Since there are no directivity-influenced records in our suite and the building is of medium height (hence first-mode dominated), the 5%-damped first-mode spectral acceleration $S_a(T_1, 5\%)$ will be our choice; it has been proven to be both efficient, by minimizing the scatter in the results, thus requiring only a few ground motion records to provide good demand and capacity estimates, and sufficient, as it provides a complete characterization of the response without the need for magnitude or distance information [4]. Similarly, selecting a *DM* can be application-specific; for example, the peak storey accelerations are well-correlated with contents' damage, while the maximum peak interstorey drift ratio θ_{\max} is known to relate well [2] to global dynamic instability and several structural performance limit-states upon which we will focus, so θ_{\max} will be our *DM* choice. Still, it cannot be emphasized enough that these choices are by no means limiting. The

user can change his mind and reprocess the IDA data anytime by choosing a different *IM* or *DM*, without any need to rerun the dynamic analyses.

Having selected our *IM* and *DM*, we are still faced with an abundance of IDA-generated data that need to be sorted out and presented in meaningful ways. It is a time-consuming and challenging task that we are going to step our way through, but it can be rendered totally effortless with the proper software. Actually, most of what follows is a direct description of the inner workings of our automated post-processing program [5], whose graphical output appears in the accompanying figures.

Generating the IDA curves by Interpolation

Once the desired *IM* and *DM* values (in our case $S_a(T_1, 5\%)$ and θ_{\max}) are extracted from each of the dynamic analyses, we are left with a set of discrete points, ten for each record, that reside in the *IM-DM* plane and lie on its IDA curve, as in Figure 1. By interpolating them, the entire IDA curve can be approximated without performing additional analyses. To do so, we may use a basic piecewise linear approximation, or the superior spline interpolation. Based on the concept of natural, coordinate-transformed, parametric splines with a centripetal scheme for knot-selection [5, 7], a realistic interpolation can be generated that accurately represents the real IDA curve, as shown in Figure 1 for record #14 of Table 1. Having the complete curve available, it is now possible to calculate *DM* values at arbitrary levels of *IM*, allowing the extraction of more *IM*, *DM* points with a minimum of computation.

The smooth IDA curve provided by the interpolation scheme offers much to observe. Even for the single record depicted in Figure 1 the IDA curve is not at all simple. It starts as a straight line in the elastic range but then shows the effect of yielding and slightly “softens” at 0.3g by displaying a tangent slope less than the elastic. Subsequently, it “hardens”, having a local slope higher than the elastic, and the building apparently responds with almost the same $\theta_{\max} \approx 3\%$ for $S_a(T_1, 5\%)$ in the range of 0.35g–0.55g. Finally, it starts softening again, showing ever increasing slopes, i.e., greater rates of *DM* accumulation as *IM* increases, reaching the “flatline” at $S_a(T_1, 5\%) \approx 0.81g$, where the structure responds with practically “infinite” θ_{\max} values and numerical non-convergence has been encountered during the analysis. That is when the building has reached global dynamic instability, when small increments in the *IM*-level result in unlimited increase of the *DM*-response.

Defining Limit-States on an IDA curve

In order to be able to do the performance calculations needed for PBEE, we need to define limit-states on the IDAs, three of which are going to be demonstrated: Immediate Occupancy, Collapse Prevention (both defined in FEMA 350 [2]) and global dynamic instability collapse. For a steel moment-resisting frame with Reduced Beam Section connections, Immediate Occupancy is violated at $\theta_{\max} = 2\%$ according to FEMA 350. On the other hand, Collapse Prevention is not exceeded on the IDA curve until the final point where the local tangent reaches 20% of the elastic slope (Figure 2) or $\theta_{\max} = 10\%$, whichever occurs first in *IM* terms. Finally, global dynamic instability happens when the flatline is reached and any increase in the *IM* results in practically infinite *DM* response. In our example of record #14 in Figure 2, Immediate Occupancy is violated for $S_a(T_1, 5\%) \geq 0.26g$ or $\theta_{\max} \geq 2\%$, while the Collapse Prevention level is exceeded if $S_a(T_1, 5\%) \geq 0.72g$ or $\theta_{\max} \geq 6.4\%$. Finally, global dynamic instability occurs at $S_a(T_1, 5\%) \geq 0.81g$, which corresponds to $\theta_{\max} = +\infty$.

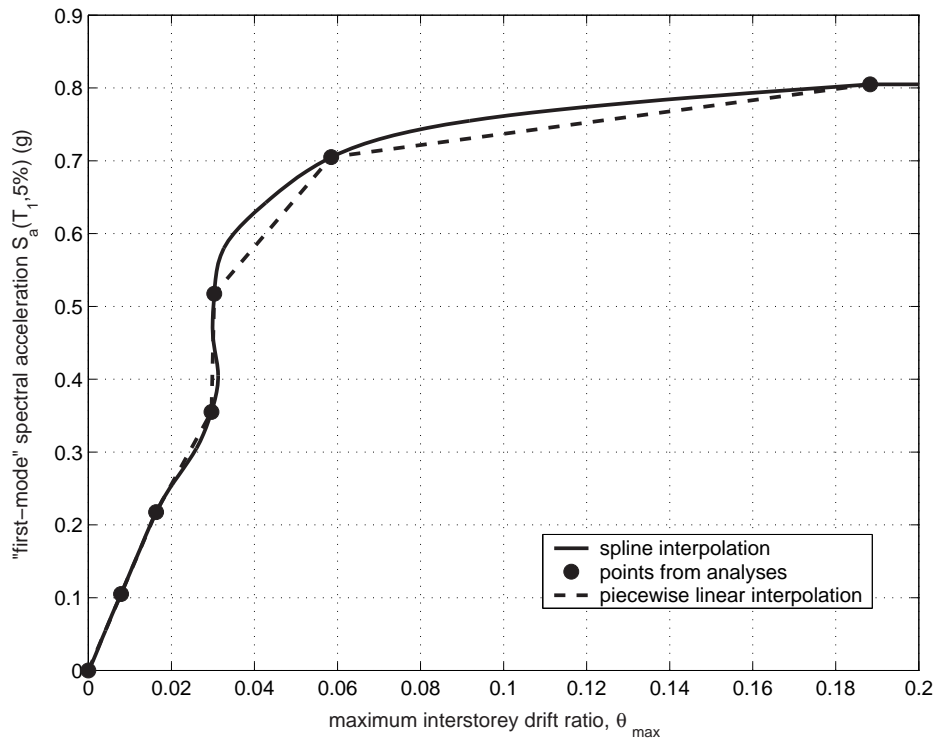


Figure 1: The six numerically-converging dynamic analysis points for record #14 are interpolated, using both a spline and a piecewise linear approximation.

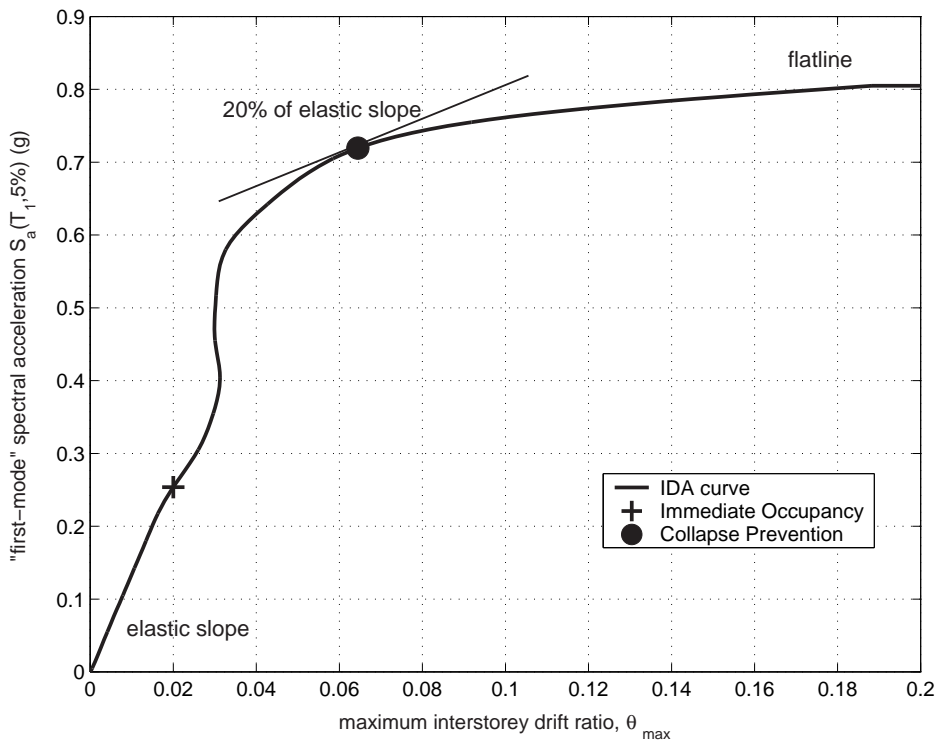


Figure 2: The limit-states, as defined on the IDA curve of record #14.

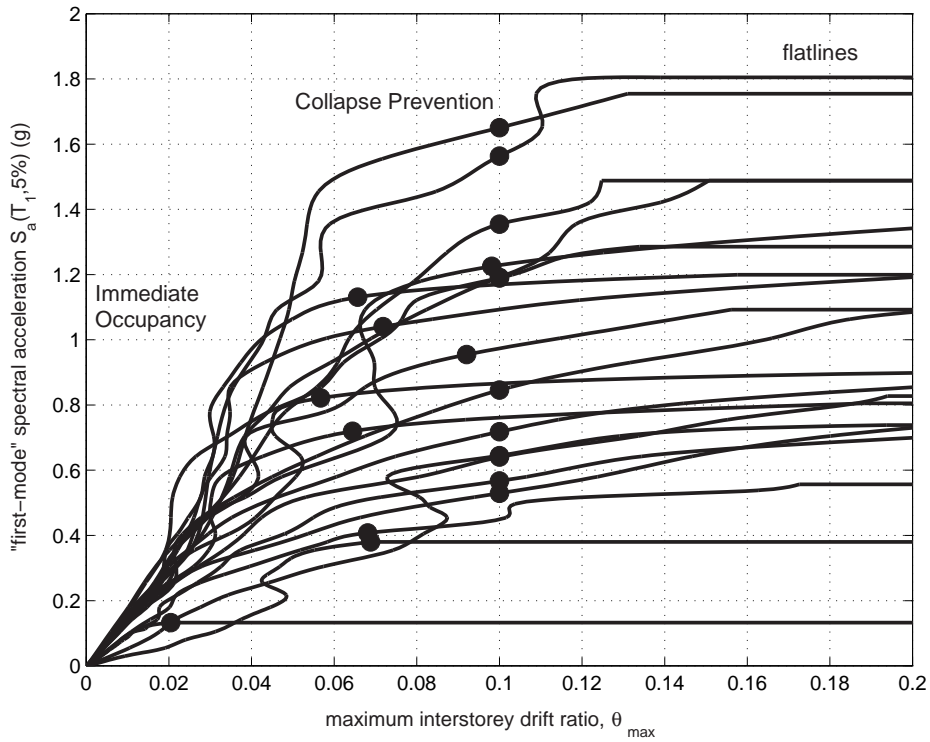


Figure 3: All twenty IDA curves and the associated limit-state capacities. The Immediate Occupancy limit is at the intersection of each IDA with the $\theta_{\max} = 2\%$ line, the Collapse Prevention limit is represented by the dots, while global dynamic instability occurs at the flatlines.

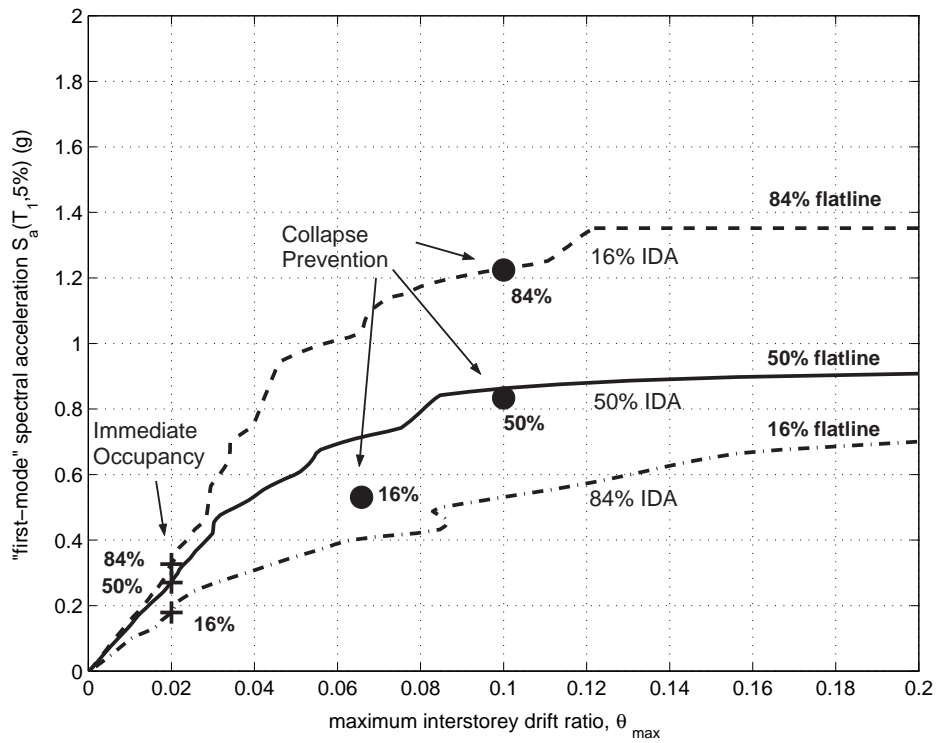


Figure 4: The summary of the IDA curves and corresponding capacities into their 16%, 50% and 84% fractiles.

Summarizing the IDAs

By generating the IDA curve for each record and subsequently defining the limit-state capacities, a large amount of data can be gathered, only part of which is seen in Figure 3. Notice the range of behavior that the IDA curves display, showing large record-to-record variability, making it essential to summarize such data and quantify the randomness introduced by the records. We need to employ appropriate summarization techniques that will reduce this data into the distribution of DM given IM and the probability of exceeding any specific limit-state given the IM level.

The limit-state capacities can easily be summarized into some central value and a measure of dispersion. Consequently, we have chosen to calculate the 16%, 50% and 84% values of DM and IM for each limit-state, as shown in Table 2, and also graphically depicted in Figure 4. For example, reading off Table 2, at $S_a(T_1, 5\%) = 0.83g$ or equivalently at $\theta_{\max} = 0.10$, 50% of the ground motion records have forced the 9-storey structure to violate Collapse Prevention.

TABLE 2
SUMMARIZED CAPACITIES FOR EACH LIMIT-STATE

	$S_a(T_1, 5\%)$ (g)			θ_{\max}		
	16%	50%	84%	16%	50%	84%
Immediate Occupancy	0.18	0.27	0.33	0.02	0.02	0.02
Collapse Prevention	0.53	0.83	1.22	0.07	0.10	0.10
Global instability	0.74	1.06	1.49	$+\infty$	$+\infty$	$+\infty$

There are several methods to summarize the IDA curves [1], but the cross-sectional fractiles is arguably the most flexible. Using the spline interpolation we can generate stripes of DM -values at arbitrary levels of $S_a(T_1, 5\%)$; each stripe contains 20 DM -values, one for each record, that may be finite or even infinite when a record has already reached its flatline at a lower IM -level. By summarizing the DM -values for each stripe into their 16%, 50% and 84% percentiles, we get fractile values of DM given IM that are in turn interpolated for each fractile to generate the 16%, 50% and 84% fractile IDA curves, shown in Figure 4. For example, given $S_a(T_1, 5\%) = 0.4g$, 16% of the records produce $\theta_{\max} \leq 2.3\%$, 50% of the records $\theta_{\max} \leq 2.5\%$ and 84% $\theta_{\max} \leq 6.5\%$. Under suitable assumptions of continuity and monotonicity of the IDA curves, the fractiles can also be used in the inverse way, e.g., in order to generate demand $\theta_{\max} = 4\%$, 84% of the records need to be scaled at levels $S_a(T_1, 5\%) \geq 0.31g$, 50% of the records at $S_a(T_1, 5\%) \geq 0.52g$ and 16% at $S_a(T_1, 5\%) \geq 0.76g$. Consequently, the 16%, 50% and 84% Immediate Occupancy points and global instability flatlines actually reside on the 84%, 50% and 16% IDA curves respectively, a direct result of the definition of these limit-states. On the other hand, no such general property exists for the Collapse Prevention points, but experience has shown that they usually lie quite close and often on top of their corresponding fractile IDAs, just like the others.

PBEE calculations

One of the goals of PBEE is producing annual rates of exceedance for the limit-states. This can be easily accomplished with the summarized results that have been calculated so far, especially if one considers the formats proposed by FEMA 350 [2] or by the Pacific Earthquake Engineering Center. The process invariably involves calculating the annual rate of exceeding values of the chosen IM , readily available for $S_a(T_1, 5\%)$ from conventional Probabilistic Seismic Hazard Analysis, and integrating with the conditional probabilities of exceeding each limit-state

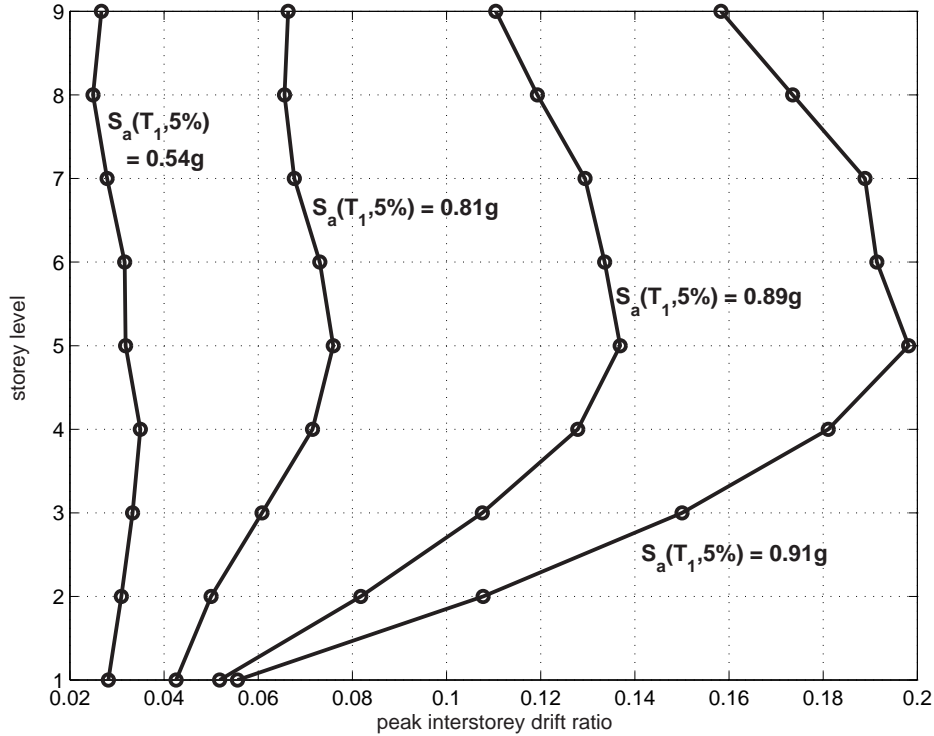


Figure 5: The median peak drifts for all storeys at several specified $S_a(T_1, 5\%)$ levels.

(given the IM level) to produce the desired annual rates of limit-state exceedance. It is a relatively straightforward method that has been described in extent, for example, by Cornell *et al.* [8].

Taking advantage of the data: SPO versus IDA

Beyond the essential calculations needed for PBEE, there is much more information that we could easily glean out of the IDA by taking a closer look at the results and plotting them in new ways. For example, Figure 5 displays a storey-to-storey profile of the median peak drifts at several $S_a(T_1, 5\%)$ -levels. As the intensity increases, then, in a median sense across all records, the 5th floor seems to accumulate most of the deformation. On the other hand, in Figure 6 the individual storey drift IDA curves are plotted for record #1, showing a record-specific picture of each storey. Most interesting for this record is the sudden change of behavior that occurs around $S_a(T_1, 5\%) = 0.82g$, when the top floors suddenly start accumulating more and more deformation as IM increases, while the previously leading lower floors are held back, displaying almost constant peak drifts.

It is also very informative to visually compare on the same figure the Static Pushover (SPO) curve (also known as the Nonlinear Static Procedure curve) versus the median (50%-fractile) IDA. Since the SPO curve usually comes in base shear versus peak roof drift coordinates, it needs to be transformed into IM and DM axes. In our case, the θ_{max} response can be easily extracted from the SPO analysis results, while the base shear can be converted to acceleration units by dividing with the building mass times some (ad hoc) factor chosen to make the curves match in their elastic range. This can be achieved for our structure by dividing the base shear with 85% of the total building mass (which is very close to the first modal mass). By thus plotting the two curves together, as pictured in Figure 7, we see that they correspond to each other. The elastic region of the IDA matches the SPO by construction, and the post-yield non-

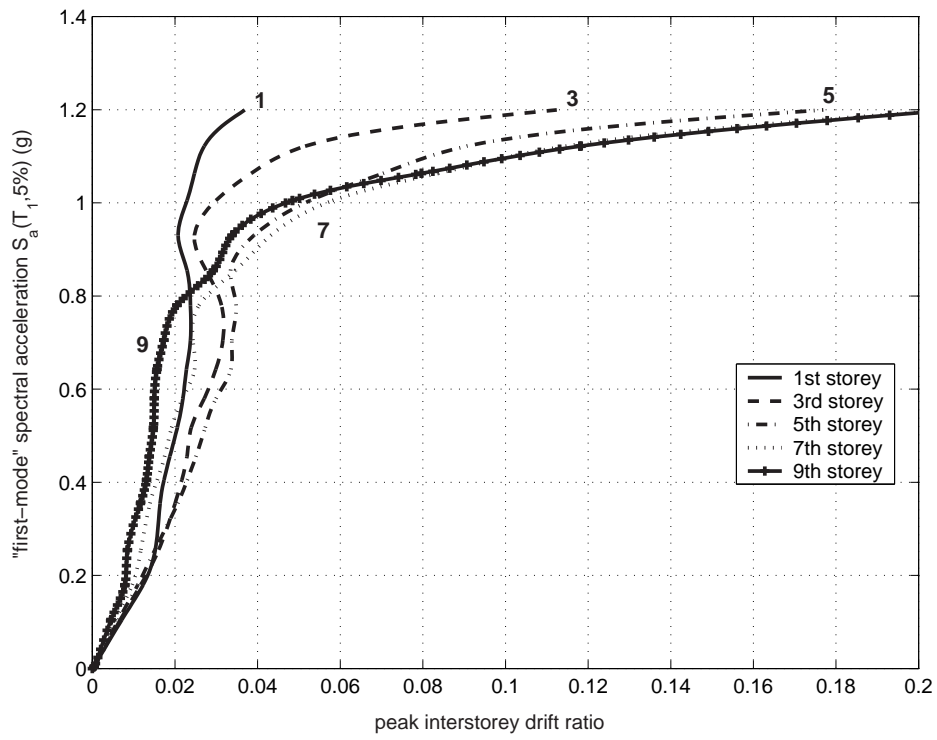


Figure 6: The IDA curves of the odd storeys for record #1.

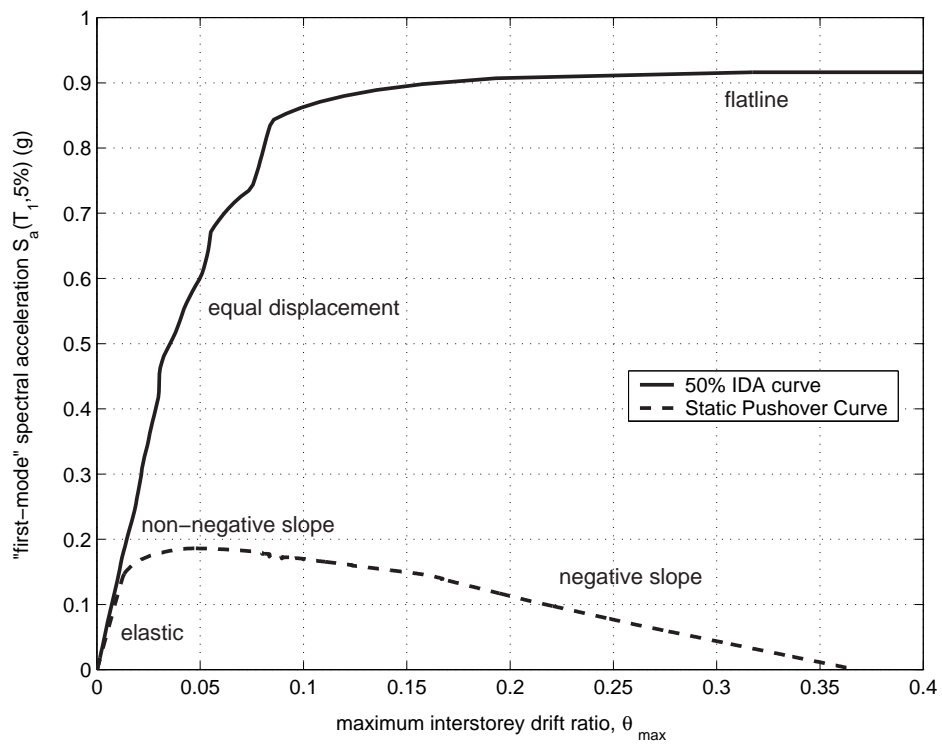


Figure 7: The SPO curve generated from a first-mode load pattern versus the median IDA.

negative SPO segment corresponds to a continuation of the elastic region in the IDA, where the IDA is following the familiar “equal displacement” rule for moderate period structures. When the SPO turns into a negative slope, the IDA softens and acquires a local slope less than the initial elastic, that gradually decreases till the IDA becomes flat. Essentially, the ending of the SPO at zero strength signals the end of the IDA by the flatline. Observing these facts, one could stipulate that some more direct, perhaps quantitative rules may be devised to connect the two curves.

CONCLUSIONS

The step-by-step application of Incremental Dynamic Analysis has been demonstrated for a 9-storey steel moment resisting frame. By using publicly available software it has become almost trivial to perform the analysis, generate the IDA curves, estimate limit-state capacities and summarize the results into a format that can be easily integrated with modern PBEE frameworks. Perhaps, the single most important thing to remember is the wealth of information that can be at our fingertips if we take advantage of ever-cheaper computing power to really dive into our structure’s behavior. Just looking at the connection of the SPO curve with the IDA or the detailed storey-by-storey behavior of the building under seismic excitation can open new directions and challenge our research.

ACKNOWLEDGEMENTS

Financial support for this research was provided by the sponsors of the Reliability of Marine Structures Affiliates Program of Stanford University.

REFERENCES

1. Vamvatsikos D, Cornell CA. Incremental dynamic analysis. *Earthquake Engineering and Structural Dynamics* 2002; 31(3): 491–514. URL http://pitch.stanford.edu/rmsweb/RMS_Papers/pdf/dimitrios/IDA-paper.pdf
2. FEMA. Recommended seismic design criteria for new steel moment-frame buildings. Report No. FEMA-350, SAC Joint Venture, Federal Emergency Management Agency, Washington DC 2000.
3. Lee K, Foutch DA. Performance evaluation of new steel frame buildings for seismic loads. *Earthquake Engineering and Structural Dynamics* 2002; 31(3): 653–670.
4. Shome N, Cornell CA. Probabilistic seismic demand analysis of nonlinear structures. Report No. RMS-35, RMS Program, Stanford University, Stanford 1999. URL <http://pitch.stanford.edu/rmsweb/Thesis/NileshShome.pdf>
5. Vamvatsikos D, Cornell CA. Tracing and post-processing of IDA curves: Theory and software implementation. Report No. RMS-44, RMS Program, Stanford University, Stanford 2002.
6. Luco N, Cornell CA. Structure-specific, scalar intensity measures for near-source and ordinary earthquake ground motions. *Earthquake Spectra* 2002; (submitted).
7. Farin G. *Curves and Surfaces for Computer Aided Geometric Design: A Practical Guide*. San Diego, CA: Academic Press, 1990, 2nd edn.
8. Cornell CA, Jalayer F, Hamburger RO, Foutch DA. The probabilistic basis for the 2000 SAC/FEMA steel moment frame guidelines. *ASCE Journal of Structural Engineering* 2002; 128(4).